nature nanotechnology

LETTERS

PUBLISHED ONLINE: 12 FEBRUARY 2012 | DOI: 10.1038/NNANO.2012.8

Intracellular recording of action potentials by nanopillar electroporation

Chong Xie[1†], Ziliang Lin[2†], Lindsey Hanson[3], Yi Cui[1,4*] and Bianxiao Cui[3*]

Action potentials have a central role in the nervous system and in many cellular processes, notably those involving ion channels. The accurate measurement of action potentials requires efficient coupling between the cell membrane and the measuring electrodes. Intracellular recording methods such as patch clamping involve measuring the voltage or current across the cell membrane by accessing the cell interior with an electrode, allowing both the amplitude and shape of the action potentials to be recorded faithfully with high signal-to-noise ratios[1]. However, the invasive nature of intracellular methods usually limits the recording time to a few hours[1], and their complexity makes it difficult to simultaneously record more than a few cells. Extracellular recording methods, such as multielectrode arrays[2] and multitransistor arrays[3], are non-invasive and allow long-term and multiplexed measurements. However, extracellular recording sacrifices the one-to-one correspondence between the cells and electrodes, and also suffers from significantly reduced signal strength and quality. Extracellular techniques are not, therefore, able to record action potentials with the accuracy needed to explore the properties of ion channels. As a result, the pharmacological screening of ion-channel drugs is usually performed by low-throughput intracellular recording methods[4]. The use of nanowire transistors[5–7], nanotube-coupled transistors[8] and micro gold-spine and related electrodes[9–12] can significantly improve the signal strength of recorded action potentials. Here, we show that vertical nanopillar electrodes can record both the extracellular and intracellular action potentials of cultured cardiomyocytes over a long period of time with excellent signal strength and quality. Moreover, it is possible to repeatedly switch between extracellular and intracellular recording by nanoscale electroporation and resealing processes. Furthermore, vertical nanopillar electrodes can detect subtle changes in action potentials induced by drugs that target ion channels.

There are two major requirements for the accurate recording of action potentials: (i) ensuring a tight seal between the cell membrane and the electrode so as to minimize signal loss to the bath medium and (ii) achieving low impedance across the cell–electrode interface to increase signal collection efficiency. Recent years have seen demonstrations of vertical nanowires forming strong interfaces with mammalian cells[13–16]. Here, we show that vertically aligned nanopillar electrodes (Fig. 1a,b) can form tight junctions with mammalian cell membranes (requirement (i)) and can lower the impedance by orders of magnitude through localized electroporation (requirement (ii)), thus achieving excellent signal strength and quality in long-term and minimally invasive extracellular and intracellular recordings.

HL-1 cells (a mouse cardiac muscle cell line[17]) cultured on nanopillar electrodes show normal growth and exhibit spontaneous beating after reaching confluence. We cultured HL-1 cells around platinum nanopillar electrodes (length, 1.5 μm; diameter, 150 nm) on glass coverslips without any underlying electrodes to examine their health by means of optical microscopy. Live imaging demonstrated that the cardiomyocytes growing on the nanopillar electrodes had a morphology similar to those on planar areas during rhythmic beating (Fig. 1c; Supplementary Movie 1). Scanning electron microscopy (SEM) after cell fixation revealed that the nanopillar electrodes were covered by the attached cell (Fig. 1d), a phenomenon similar to that observed previously in nanostructure–cell interactions[9,13,14]. To further inspect the cell–nanopillar electrode interface, we used focused ion beam (FIB) milling to expose the interface cross-section. Subsequent SEM imaging revealed that the nanopillar electrodes were engulfed tightly by the cell (Fig. 1e). Protrusions from the cells growing next to the nanopillar electrodes demonstrated a strong tendency to attach to the nanopillar electrodes (Fig. 1f), suggesting strong interactions between these electrodes and the cell membrane. Our findings agree with those of our previous study on the interaction between platinum nanopillars and primary cultured rat neurons[15].

Devices assembled with the nanopillar electrode arrays (typically nine nanopillars per array with underlying electrical connections) were then used to record action potentials from HL-1 cardiomyocytes. Figure 2a shows that the recorded action potential exhibits two signatures of extracellular recording: a spike with a shape that corresponds to the first derivative of the intracellular potential and an amplitude of ~100–200 μV. The peak-to-peak noise level is 30 μV_{pp} and the signal-to-noise ratio is in the range 4.5–9. For comparison, a typical commercial multielectrode array registers a noise level of 40 μV_{pp} for TiN electrodes with a diameter of 10 μm and 10 μV_{pp} for a diameter of 30 μm, and an action potential signal strength of 100–500 μV. It is important to note that although the signal strength recorded by the nanopillar electrode arrays is similar to that measured by commercial planar multielectrode arrays, the surface area of a nanopillar electrode array (5–10 μm^2) is much smaller than that of a multielectrode array (400–2,500 μm^2)[2]. Because of the capacitive coupling nature of a solid-state electrode, the detected signal strength directly correlates with the electrode area. Our observation suggests that tight engulfment of the nanopillar electrodes by the cell membrane results in good sealing at the interface and therefore compensates for the decreased electrode detection area.

A transient electroporation drastically improves the quality of the nanopillar electrode-recorded signal by lowering the impedance between the electrode and the cell interior. A high electric field can induce nanometre-sized pores in the cell membrane, as in the

[1]Department of Materials Science and Engineering, Stanford University, Stanford, California 94305, USA, [2]Department of Applied Physics, Stanford University, Stanford, California 94305, USA, [3]Department of Chemistry, Stanford University, Stanford, California 94305, USA, [4]Stanford Institute for Materials and Energy Sciences, SLAC National Accelerator Laboratory, 2575 Sand Hill Road, Menlo Park, California 94025, USA, †These authors contributed equally to this work. *e-mail: bcui@stanford.edu; yicui@stanford.edu

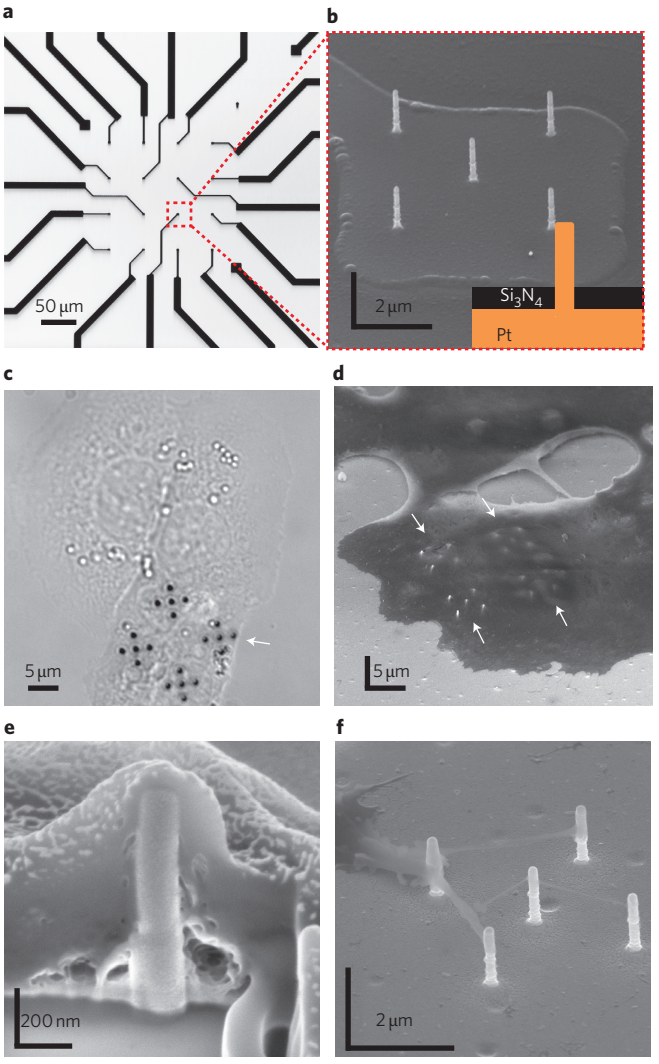

Figure 1 | Nanopillar electrode devices and their interactions with HL-1 cardiomyocytes. a, Optical image of a nanopillar electrode device with a four-by-four array of platinum pads and leads connected to recording amplifiers. **b**, SEM image of an array of five vertical nanopillar electrodes on one of the platinum pads: the electrodes are 1.5 µm tall and have a diameter of 150 nm. The footprint of the nanopillar electrode array on each pad is 5×5 µm^2 or less. The pads and leads are electrically insulated by a 350 nm Si_3N_4/SiO_2 layer. Most of the surface of the nanopillars is exposed for electrical detection. Inset: schematic of a nanopillar electrode. **c**, Optical image of HL-1 cells cultured on a glass coverslip with four arrays of electrodes (each array contains five nanopillars). There are no underlying platinum pads in this sample. The morphology of cells grown on vertical nanopillar electrodes is similar to the morphology of cells grown on planar subtrates. **d**, SEM image showing four five-electrode arrays covered by an HL-1 cell. Arrows indicate the locations of nanopillar electrodes. **e**, The cell–nanopillar electrode interface exposed by FIB milling shows that the nanopillar electrode is fully engulfed by the cell. **f**, SEM image showing cellular protrusions reaching out to the nanopillar electrodes. All SEM images are taken at 52° to normal.

established *in vitro* technique that uses electroporation to introduce DNA or other molecules into cells[18–20]. Because our electrodes are sharp (tip radius of <100 nm) and tightly coupled to the membrane, they can create a large electric field with a small voltage to transiently and locally increase the permeability of the cell membranes (Fig. 2c). Figure 2b shows the recorded action potentials after the nanopillar electrodes deliver a train of 2.5 V, 200 µs biphasic pulses

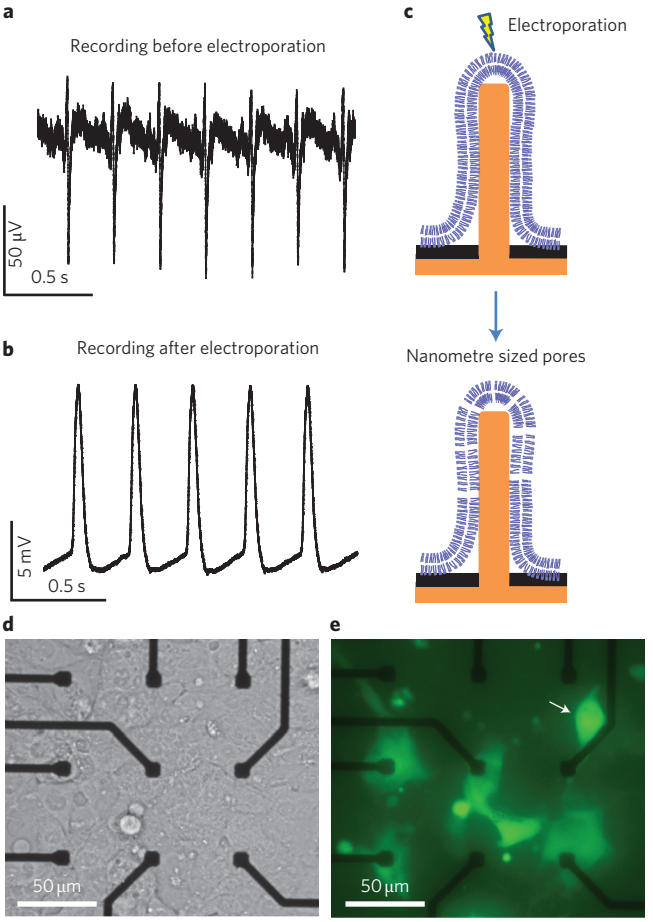

Figure 2 | Recording action potentials of a single HL-1 cell before and after electroporation. a, Before electroporation, the recorded train of action potentials shows extracellular signatures. **b**, After electroporation, the recorded signal amplitude increases by a factor of >100 and the shape exhibits intracellular features. Note that the *y*-axes in **a** and **b** have different scales. **c**, Schematic (not to scale) of the electroporation of the cell membrane by a nanopillar electrode. Voltage pulses create nanoscale pores in the region of the cell membrane that surrounds the nanopillar electrode. **d**,**e**, To confirm that nanopillar electroporation has taken place, confluent HL-1 cells are cultured on a three-by-three array of platinum pads in which the six pads in the second and third rows contain arrays of nine nanopillar electrodes, but the three pads in the top row contain milled holes but no nanopillars. We then introduce calcein, a membrane-impermeable dye, and perform electroporation. Comparison of the bright-field (**d**) and fluorescence (**e**) images of the same area confirms that the calcein dye only enters those cells that contact the nanopillar electrodes. No electroporation is observed on the top three control pads. Moreover, each array of nine nanopillar electrodes interfaces with just one cell. The cell on the top right (white arrow) is not directly over the electrode, but its membrane protrusion extends to the nearest nanopillar electrode site (Supplementary Fig. S2).

(20 pulses in 1 s) to an HL-1 cell. The recorded signal amplitude increases to 11.8 mV immediately after electroporation. The noise level of 30 µV_{pp} is similar to that of extracellular recording levels, but the signal-to-noise ratio increases to 590 (Fig. 2b versus Fig. 2a). In comparison, a typical current-clamp recording has a noise level of 180 µV_{rms} and signal strength of ~100 mV (ref. 1). Nanowire field-effect transistors typically have a noise level of 2–3 mV and signal of 60 mV (ref. 6). In addition to this 100-fold increase in the signal-to-noise ratio, our recorded action potentials have the following intracellular attributes: a triangular shape and action potential duration at 50% of the maximum (APD50) of 30.8±0.2 ms.

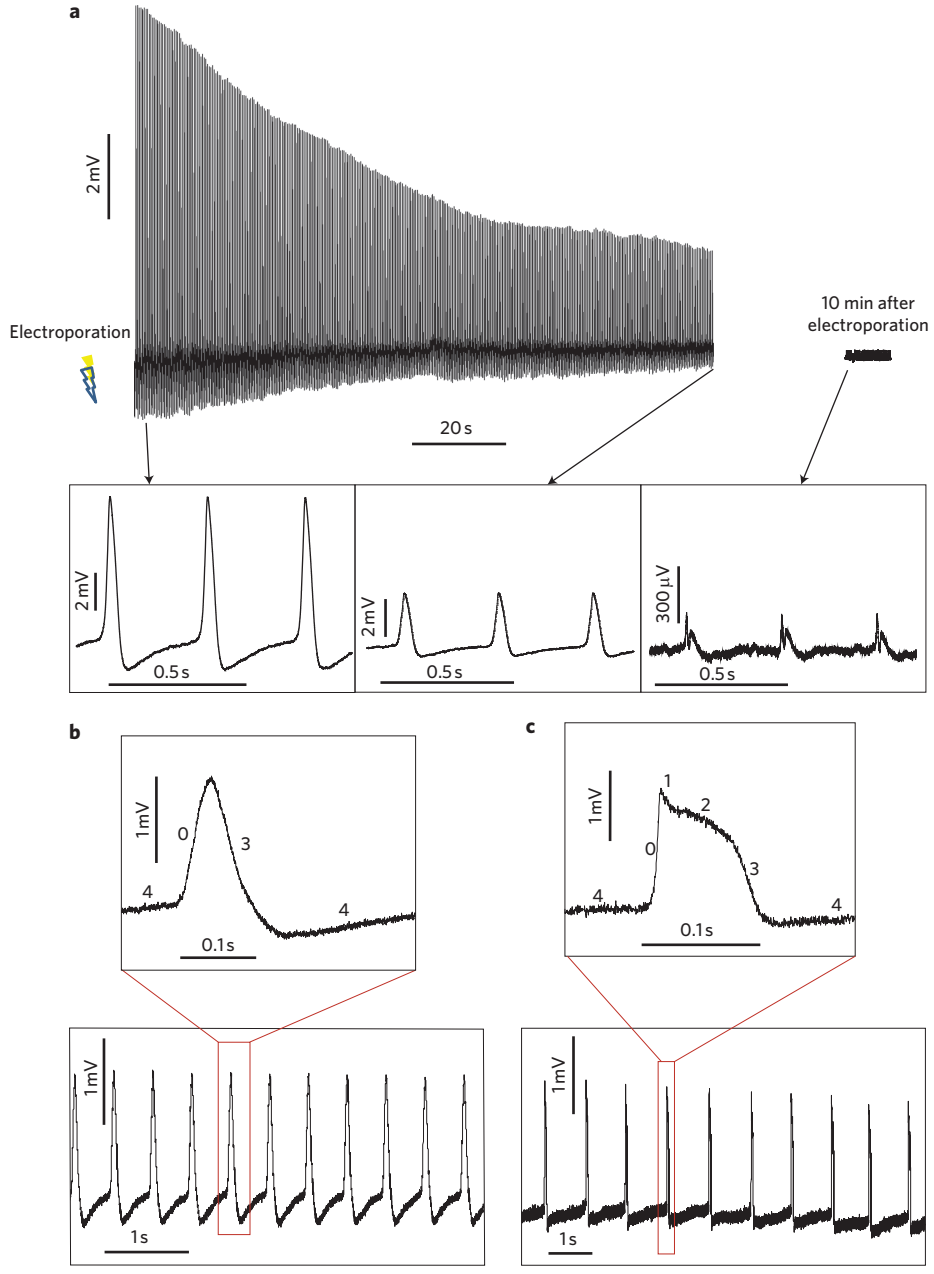

Figure 3 | Minimally invasive intracellular measurement of action potentials with high precision. a, After electroporation, the recorded action potential amplitude decays over time due to sealing of transient pores in the cell membrane. At 120 s after electroporation, the amplitude decays to 30% of its maximum value, but APD50 remains constant during this period (Supplementary Fig. S3). About 10 min after electroporation, the recorded signal approaches an extracellular amplitude and shape. Three different segments of the recording are enlarged for clarity. The sealing of the cell membrane indicates that the intracellular recording is only invasive over a very short period of time compared to the lifetime of the cell in the culture. **b**,**c**, Intracellular recording of action potentials of two types of HL-1 cells that are designated as pacemaker (**b**) and non-pacemaker (**c**) based on their shapes. Although the recorded amplitude decays, all five phases of the non-pacemaker action potential can still be readily observed 400 s after electroporation. In contrast, the pacemaker action potentials exhibit three phases with symmetric rising and falling edges.

Immediately following each action potential, a clear refractory period is visible, which is characterized by a slow smooth transition from the maximum diastolic potential to the threshold for the initiation of the next action potential. The recorded action potential shape agrees well with patch-clamp recording of HL-1 cells[21]. A total of 32 devices with at least two cultures on each device were tested, and intracellular recording after electroporation was observed for every culture on every device.

Electroporation was confirmed by delivering membrane-impermeable calcein dye into the HL-1 cells with the same pulse sequence used to induce intracellular recording (Fig. 2d,e). Of the nine platinum pads shown in Fig. 2d (the nanopillar electrodes on the pads are not visible in this image, which was taken by an inverted microscope), the six pads in the second and third rows have nanopillar electrode arrays. To serve as a control, the three pads in the topmost row had milled holes to expose the platinum pads, but no nanopillar electrodes. As shown in Fig. 2e, although the same pulse sequence was applied to all nine platinum pads, only those cells on nanopillar electrode arrays experienced electroporation and took up the dye. Notably, not all the permeabilized cells were located exactly on top of the nanopillar electrodes. The cell indicated by the white arrow in Fig. 2e is not directly over the

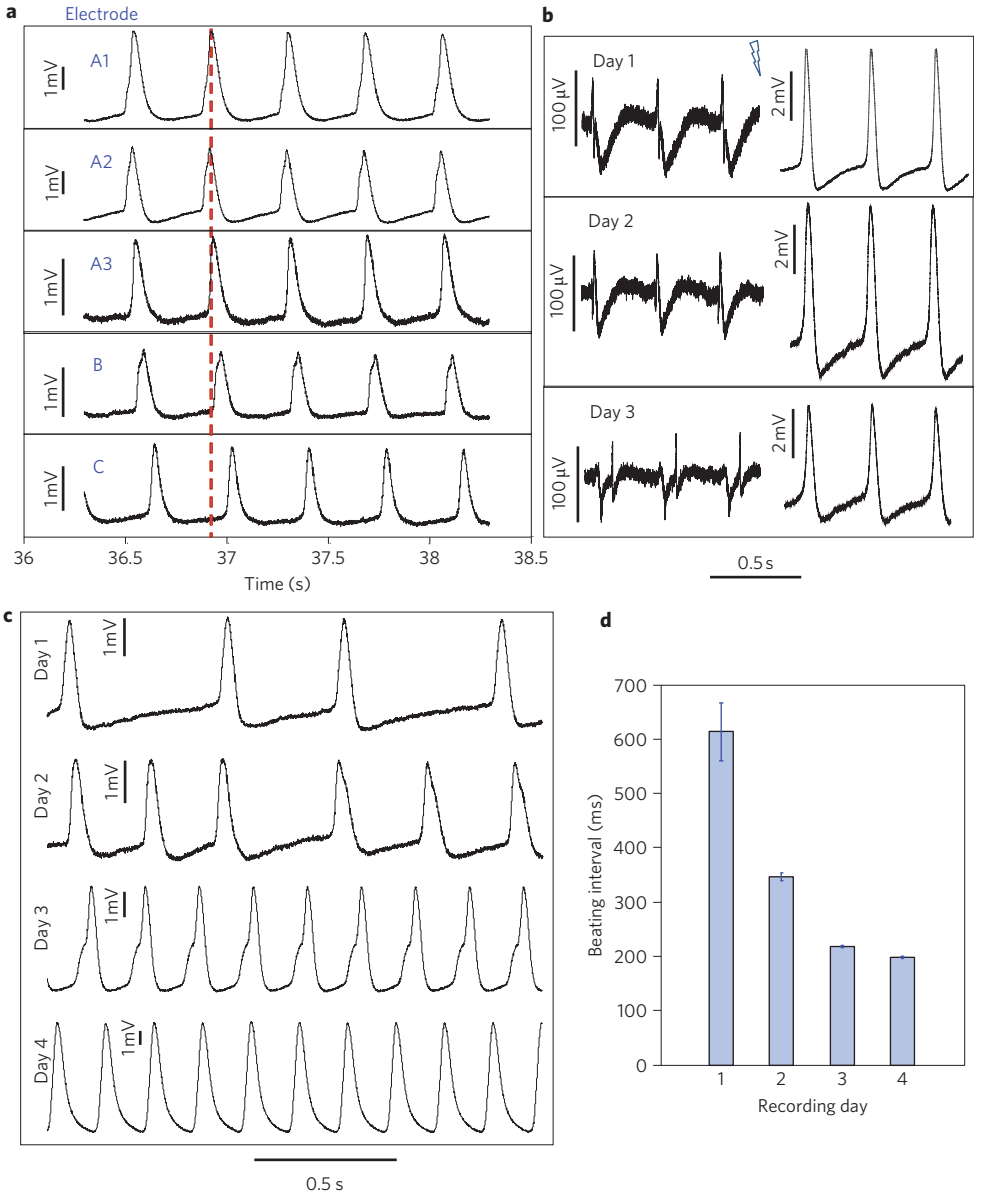

Figure 4 | Parallel intracellular recording of multiple cells and the evolution of action potentials over consecutive days for single cells. a, Simultaneous intracellular recording with five different electrodes on the same culture. Electrodes A1, A2 and A3 are within 40 μm of one another, and electrodes B and C are separated by ~400 μm from one another and from electrodes A1–A3. Cardiomyocytes on electrodes A1–A3 undergo synchronized beating, but there are time delays with cardiomyocytes on electrodes B and C. The dotted red line representing the same time is drawn to guide the eye. **b**, Extracellular (left) and intracellular (right) recording of a mature HL-1 cell over consecutive days. The shape and amplitude of the action potential exhibit minimal changes. Note that the *y*-axes on the left and right have different scales. **c**, Intracellular recording of an HL-1 cell in a developing culture over four consecutive days. We observe a transition from arrhythmic to rhythmic beating, a decrease in the beating interval, a significant change in the action potential shape and an increase in the maximum amplitude of the recorded action potential. (Note that the *y*-axes on the four traces have different scales.) **d**, Histogram showing how the beating interval decreases from day 1 to day 4. (The 23 action potentials recorded immediately after each electroporation were analysed; error bars represent one standard deviation.).

electrode, but, like the cell shown in Fig. 1f, its protrusion extends to the nearest nanopillar electrode site (as can be seen in the image with higher contrast in Supplementary Fig. S2). It is important to note that nanopillar electrode electroporation causes minimal cell damage because a relatively low voltage is applied, and electroporation happens only in the membrane immediately surrounding each electrode, which has an area of ~1 μm^2 (compared to the overall cell membrane area of ~1,000 μm^2).

Nanopillar electrode intracellular recording following electroporation is not only minimally invasive but also provides details of HL-1 action potentials with high resolution. We observe that electroporation-generated pores seal within several minutes. Figure 3a shows a 10 min recording immediately after electroporation. The amplitude of the recorded action potential decays to 30% of its original amplitude after 120 s. However, during this period, the APD50 remains relatively constant (Supplementary Fig. S3). After 10 min, the recorded signal decays to ~200 μV and transitions back to extracellular features. The timescale for pore sealing is comparable to that of the recovery reported after the electroporation of bulk suspended cells[22]. This observation further confirms that the recorded signal improvement is a direct result of electroporation. In addition, the high-resolution recording allows

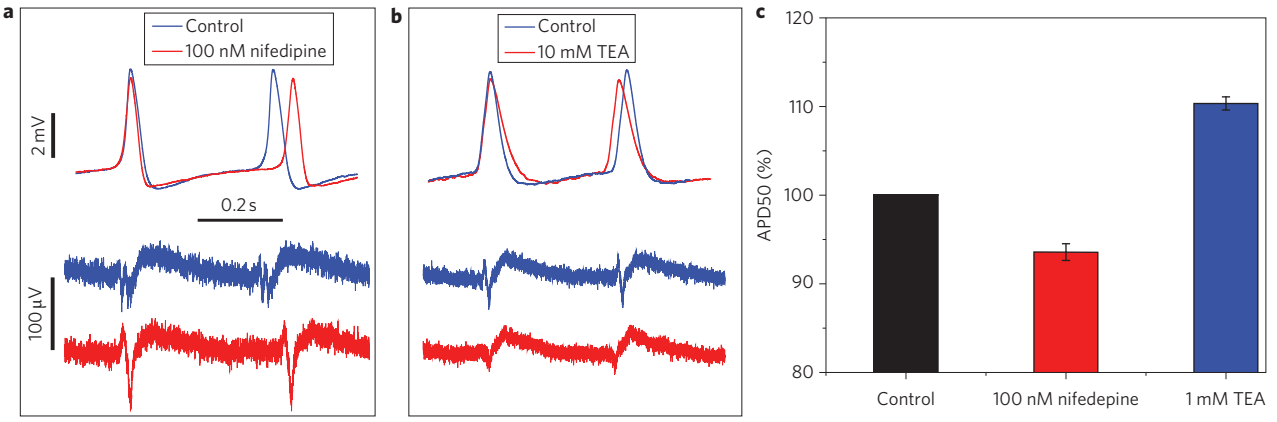

Figure 5 | Effect of ion-channel blocking drugs on HL-1 cells. a, Extracellular action potentials recorded by nanopillar electrodes (bottom), and intracellular action potentials recorded by nanopillar electrodes after electroporation (top) after nifedipine (a Ca^{2+} channel blocker) is administered to HL-1 cells (red lines). Changes in the duration and period of the action potential with respect to a control experiment (blue line) are much clearer in the intracellular recordings. **b**, Similar results are found when tetraethylammonium (a K^+ channel blocker) is administered. The rising edges of the first action potential in each pair of traces are overlaid to allow comparison (note that the vertical scale bars are different). **c**, Nifedipine leads to a reduction in the APD50 relative to the control, and tetraethylammonium (TEA) leads to an increase. For each drug, four different HL-1 cells on three different cultures are measured (see Supplementary Tables 1 and 2 for further details).

the possibility of distinguishing different types of cells in the same culture based on the shapes of their action potentials. For example, the action potential shown in Fig. 3b resembles that of pacemaker cells, whereas the action potential shown in Fig. 3c resembles that of non-pacemaker cells. The pacemaker cells have three phases with symmetric rising and falling edges. The slow rising edge is phase 0, attributed to increased inward Ca^{2+} conductance, and the falling edge is phase 3, caused by K^+ channel opening. In contrast, all five phases are present in non-pacemaker cells. The five phases represent, respectively, the opening of fast Na^+ channels (depolarization phase 0), the transient outwards K^+ channels (short repolarization phase 1), the slow inward Ca^{2+} channels (plateau phase 2) and the K^+ channels (depolarization phase 3 and resting potential phase 4).

The high-throughput and minimally invasive character of nanopillar electrode intracellular recording allows repetitive recording on multiple cells, in parallel, over several consecutive days. Figure 4a shows simultaneous intracellular recording with five different electrodes on the same culture. Electrodes A1, A2 and A3 are within 40 μm of one another, and electrodes B and C are separated by ~400 μm from one another and from electrodes A1–A3. We observe that cells on electrodes A1–A3 undergo synchronized beating, but there are time delays between cells on electrodes B and C. This is probably because different cell patches in the culture beat with delays before they reach confluence and start synchronized beating.

Figure 4b shows recordings from a cell in a mature culture on three consecutive days before and after each electroporation. Although the amplitude of the recorded signal varies, the recorded action potential shape, APD50 and frequency remain relatively constant over the three-day period. In contrast, an HL-1 cell in a developing culture exhibits significant changes in both beating interval and action potential amplitude over the course of four days (Fig. 4c). The cell transitions from arrhythmic to rhythmic beating with increasing frequency (beating interval of 613.2 ± 53.6 ms on day 1 and 197.8 ± 0.5 ms on day 4; Fig. 4d), together with an increase in recorded maximum action potential amplitude (2.76 mV on day 1 and 9.49 mV on day 4).

The highly detailed recording by the nanopillar electrodes after electroporation also allows us to examine the effect of ion-channel drugs on HL-1 action potentials. We demonstrated this capability as an example of potential drug screening applications by testing nifedipine (a Ca^{2+} channel blocker that shortens action potentials) and tetraethylammonium (a K^+ channel blocker that lengthens action potentials)[23–25]. For control experiments, we electroporated the cells to record action potentials in the absence of drugs. After the cells had recovered for a few hours, nifedipine or tetraethylammonium of different concentrations was added to the culture medium and the cultures incubated for 10 min. Subsequently, another electroporation was applied to record the action potentials of the drug-treated cells. As shown in Fig. 5, nanopillar electroporation recording revealed subtle changes in the shape, duration and frequency of the action potentials. Treatment with 100 nM nifedipine clearly decreases the duration of the action potential (quantified by APD50) and increases the period. Treatment with 10 mM tetraethylammonium shows the opposite effect, increasing APD50 and decreasing the period. For either drug, the effects on APD50 and action potential period are enhanced with increasing concentration (Supplementary Fig. S4). Although the shapes of recorded action potentials vary from cell to cell, the drug effect was reliably detected because we were taking recordings from the same cell before and after drug application (Supplementary Tables 1 and 2).

With the advantages of long-term measurement, high sensitivity and minimal invasiveness, vertical nanopillar electrode recording has many potential applications, including basic biomedical research (for example, studying the electrophysiology of different domains within single cells or groups of cells, and investigating the evolution of individual cell electrophysiology during cell development) and pharmaceutical screening. Moreover, unlike existing recording techniques, arrays of nanopillar electrodes can be used to mechanically pin down mammalian cells[15], which should allow targeted cells to be measured without chemical or biological labels.

Methods

Chemicals and reagents. Four-inch quartz wafers were purchased from Hoya Optics. Chromium etchant CR14 was sourced from Transene. All reagents used for cell culture, including gelatin, fibronectin, Claycomb medium, fetal bovine serum, norepinephrine, L-glutamine, penicillin and streptomycin, were purchased from Sigma-Aldrich, as well as ion channel drugs, nifedipine and tetraethylammonium. SEM sample preparation supplies such as glutaraldehyde, sodium cacodylate buffer and osmium tetroxide were bought from Ted Pella. RTV108 silicone glue was from Momentive.

Nanopillar electrode device fabrication and characterization. A four-inch quartz wafer was diced into 20 × 20 mm^2 pieces, and each piece was patterned with

four-by-four electrode (Pt/Ti, 100 nm/10 nm) leads and pads using standard photolithography methods. The custom-designed electrode pattern is shown in Fig. 1a and Supplementary Fig. S1a. The substrate surface was passivated with a 350 nm Si_3N_4/SiO_2 layer deposited by plasma-enhanced chemical vapour deposition. After coating with 5 nm chromium, a focused gallium ion beam was used to mill 250-nm-diameter holes through the insulation layer to reach the platinum pads underneath (FEI Strata DB 235). Vertical nanopillar electrodes were then created from the holes with FIB-assisted platinum and electrically connected with the platinum pads under the insulation layer. For each platinum pad, 1–10 nanopillar electrodes were constructed. Each nanopillar electrode was 1–2 μm long, with a diameter of 150–200 nm. After nanopillar electrode fabrication, the chromium layer was removed by CR14 so that the substrate was transparent, except for the electrode-covered areas. The electrical impedance of a finished chip in Claycomb culture medium was measured with an Agilent B1500A parameter analyser, and was shown to decrease as the number of nanopillar electrodes increases (Supplementary Fig. S5). A plastic chamber was glued onto the centre of the chip using RTV108 silicone glue for cell culture purposes. The device was finished by mounting the chip on a custom-designed printed circuit board and electrically connecting it by wire bonding (Supplementary Fig. S1).

HL-1 cell culture and optical imaging. The HL-1 cardiomyocyte cell line was obtained from the laboratory of William C. Claycomb at Louisiana State University. Before plating, the nanopillar electrode device was cleaned with detergent and deionized water, followed by 5 min of oxygen plasma treatment. The culture chamber was coated with 5 μg ml^{-1} fibronectin in 0.02% gelatin solution overnight to facilitate cell attachment[17]. HL-1 cells were then plated inside the chamber at a density of ~1×10^5 cm^{-2} and maintained in the Claycomb medium supplemented with 10% fetal bovine serum, 0.1 mM norepinephrine, 2 mM L-glutamine and 100 U ml^{-1} penicillin and 100 μg ml^{-1} streptomycin. The cells were maintained in a standard incubator at 37 °C and 5% CO_2. Medium was changed every 24 h. A typical HL-1 cell culture reaches confluence 4–5 days after plating and exhibits spontaneous and synchronous beating, which can be observed on a Leica DM6000 inverted microscope (Supplementary Movie). Fluorescent imaging of calcein dye was performed with a 470 nm excitation filter and a 525 nm emission filter.

SEM/FIB sample preparation. HL-1 cells cultured on the nanopillar electrodes were fixed with 2% glutaraldehyde and 4% paraformaldehyde in 0.1 M cacodylate buffer (pH 7.3), washed in the same buffer, and post-fixed with 1% osmium tetroxide. After washing twice in deionized water, the sample was dehydrated by successive exchanges with increasing concentrations of ethanol (50%, 70%, 90% and 100%). The sample in 100% ethanol was dried with liquid CO_2 in a critical point drier, which preserved the cell morphology during the drying step. Before SEM imaging, the sample was sputter-coated with a 2 nm gold layer to improve conductance. The sample was imaged using a FEI Strata 235B dual-beam SEM/FIB system that combined high-resolution SEM imaging and FIB milling. To expose the cell–nanopillar electrode interface, a cell-covered nanopillar electrode was first located under SEM, and FIB was used to carry out submicrometre vertical dissection at the desired locations.

Electrophysiology measurement. A 60-channel voltage amplifier system (Multichannel System, MEA1060) was used to record HL-1 cells cultured on the nanopillar electrode arrays (nine nanopillars per array) after the cells started beating. Recording was performed in the same culture medium at 37 °C with a Ag/AgCl electrode in the medium as the reference electrode. The amplification was typically 110× for intracellular recording or 1,100× for extracellular recording, and the sampling rate was 5–20 kHz. The signal was filtered with a band-pass of 1 Hz–5 kHz. For electroporation, 20 biphasic pulses of 2.5 V_{amp} were applied to a nanopillar electrode in a total time of 1 s. The recording system was blanked during the electroporation period. Electrophysiology recordings were resumed 20–40 s after electroporation to avoid amplifier saturation.

Received 14 December 2011; accepted 9 January 2012; published online 12 February 2012

References

1. Sakmann, B. & Neher, E. *Single-Channel Recording*, 2nd edn (Springer, 2009).
2. Pine, J. Recording action potentials from cultured neurons with extracellular microcircuit electrodes. *J. Neurosci. Methods* **2,** 19–31 (1980).
3. Lambacher, A. *et al.* Electrical imaging of neuronal activity by multi-transistor-array (MTA) recording at 7.8 μm resolution. *Appl.Phys. A* **79,** 1607–1611 (2004).
4. Zheng, W., Spencer, R. H. & Kiss, L. High throughput assay technologies for ion channel drug discovery. *Assay Drug Dev. Technol.* **2,** 543–552 (2004).
5. Timko, B. P. *et al.* Electrical recording from hearts with flexible nanowire device arrays. *Nano Lett.* **9,** 914–918 (2009).
6. Tian, B. *et al.* Three-dimensional, flexible nanoscale field-effect transistors as localized bioprobes. *Science* **329,** 830–834 (2010).
7. Qing, Q. *et al.* Nanowire transistor arrays for mapping neural circuits in acute brain slices. *Proc. Natl Acad. Sci. USA* **107,** 1882–1887 (2010).
8. Duan, X. *et al.* Intracellular recordings of action potentials by an extracellular nanoscale field-effect transistor. *Nature Nanotech.* http://doi: dx.doi.org/10.1038/nnano.2011.223 (2011).
9. Hai, A., Shappir, J. & Spira, M. E. In-cell recordings by extracellular microelectrodes. *Nature Methods* **7,** 200–202 (2010).
10. Hai, A., Shappir, J. & Spira, M. E. Long-term, multisite, parallel, in-cell recording and stimulation by an array of extracellular microelectrodes. *J. Neurophysiol.* **104,** 559–568 (2010).
11. Braeken, D. *et al.* Local electrical stimulation of single adherent cells using three-dimensional electrode arrays with small interelectrode distances. *Conf. Proc. IEEE Eng. Med. Biol. Soc.* **2009,** 2756–2759 (2009).
12. Choi, D. S. *et al.* Detection of neural signals with vertically grown single platinum nanowire-nanobud. *J. Nanosci. Nanotechnol.* **9,** 6483–6486 (2009).
13. Kim, W., Ng, J. K., Kunitake, M. E., Conklin, B. R. & Yang, P. Interfacing silicon nanowires with mammalian cells. *J. Am. Chem. Soc.* **129,** 7228–7229 (2007).
14. Shalek, A. K. *et al.* Vertical silicon nanowires as a universal platform for delivering biomolecules into living cells. *Proc. Natl Acad. Sci. USA* **107,** 1870–1875 (2010).
15. Xie, C. *et al.* Noninvasive neuron pinning with nanopillar arrays. *Nano Lett.* **10,** 4020–4024 (2010).
16. Xie, C., Hanson, L., Cui, Y. & Cui, B. Vertical nanopillars for highly localized fluorescence imaging. *Proc. Natl Acad. Sci. USA* **108,** 3894–3899 (2011).
17. Claycomb, W. C. *et al.* HL-1 cells: a cardiac muscle cell line that contracts and retains phenotypic characteristics of the adult cardiomyocyte. *Proc. Natl Acad. Sci. USA* **95,** 2979–2984 (1998).
18. Zimmermann, U., Pilwat, G. & Riemann, F. Dielectric breakdown of cell membranes. *Biophys. J.* **14,** 881–899 (1974).
19. Neumann, E., Schaeferridder, M., Wang, Y. & Hofschneider, P. H. Gene-transfer into mouse lyoma cells by electroporation in high electric-fields. *EMBO J.* **1,** 841–845 (1982).
20. Chang, D. C. & Reese, T. S. Changes in membrane structure induced by electroporation as revealed by rapid-freezing electron microscopy. *Biophys. J.* **58,** 1–12 (1990).
21. Sartiani, L., Bochet, P., Cerbai, E., Mugelli, A. & Fischmeister, R. Functional expression of the hyperpolarization-activated, non-selective cation current $I(f)$ in immortalized HL-1 cardiomyocytes. *J. Physiol.* **545,** 81–92 (2002).
22. Tovar, O. & Tung, L. Electroporation and recovery of cardiac cell membrane with rectangular voltage pulses. *Am. J. Physiol.* **263,** H1128–H1136 (1992).
23. Zipes, D. P. & Jalife, J. *Cardiac Electrophysiology : From Cell to Bedside*, 4th edn (Saunders, 2004).
24. Catterall, W. A. Structure and function of voltage-sensitive ion channels. *Science* **242,** 50–61 (1988).
25. Choi, K. L., Aldrich, R. W. & Yellen, G. Tetraethylammonium blockade distinguishes two inactivation mechanisms in voltage-activated K^+ channels. *Proc. Natl Acad. Sci USA* **88,** 5092–5095 (1991).

Acknowledgements

The HL-1 cardiac cell line was obtained from William C. Claycomb (Louisiana State University). This work was supported by the NSF (CAREER award no. 1055112), the NIH (grant no. NS057906), a Searle Scholar award, a Packard Science and Engineering Fellowship (to B.C.) and a National Defense Science and Engineering Graduate Fellowship (to Z.L.)

Author contributions

All authors conceived the experiments. C.X., Z.L. and L.H. carried out experiments. All authors contributed to the scientific planning, discussions and writing of the manuscript.

Additional information

The authors declare no competing financial interests. Supplementary information accompanies this paper at www.nature.com/naturenanotechnology. Reprints and permission information is available online at http://www.nature.com/reprints. Correspondence and requests for materials should be addressed to Y.C. and B.C.